Acta Crystallographica Section D
Biological Crystallography
ISSN 0907-4449

Structures of the human ceramide activator protein saposin D

Konstantin Popovic[a] and Gilbert G. Privé[a,b,c]*

[a]Department of Medical Biophysics, University of Toronto, Toronto, Ontario, Canada, [b]Department of Biochemistry, University of Toronto, Toronto, Ontario, Canada, and [c]Division of Cancer Genomics and Proteomics, Ontario Cancer Institute, Toronto, Ontario M5G 1L7, Canada

Correspondence e-mail: prive@uhnres.utoronto.ca

Received 28 November 2007
Accepted 28 January 2008

PDB References: saposin D, orthorhombic, 3bqp, r3bqpsf; triclinic, 3bqq, r3bqqsf.

Saposin D is a sphingolipid activator protein required for the lysosomal breakdown of ceramide to a fatty acid and sphingosine by acid ceramidase. The crystal structure of saposin D has been determined in two different crystal forms, resulting in a total of six crystallographically independent views of this small 80-amino-acid protein. All of the structures are highly similar and reveal the monomeric form of the saposin fold previously seen in the crystal structures of saposins A and C. Saposin D is slightly more compact than the related saposins A and C owing to a slight repositioning of the 'stem' and 'hairpin' regions of the protein.

1. Introduction

Sphingolipids (SLs) are essential components of eukaryotic cell membranes, with roles in cell adhesion, cell growth, cell regulation, intracellular trafficking and interactions with signal molecules and toxins (Sandhoff & Kolter, 2003; Watts, 2003). Typically, two proteins are involved in the lysosomal breakdown of an SL: an acid hydrolase and an activator protein. If either protein is functionally absent, the corresponding lipid substrate accumulates and is stored within tissues of the body (Futerman & van Meer, 2004). Although the more common forms of lipid-storage diseases arise from the loss of a particular hydrolase enzyme, cases where there is normal hydrolase activity but no observable activator protein demonstrate the essential role played by the activator proteins (Kolter & Sandhoff, 2005). One specific class of activator proteins are the saposins; saposin D is required to activate the hydrolysis of ceramide to a fatty acid and sphingosine by acid ceramidase *in vitro* and *in vivo* (Azuma *et al.*, 1994; Klein *et al.*, 1994; Linke *et al.*, 2001). The loss of acid ceramidase activity results in the abnormal accumulation of ceramide and presents clinically as Farber disease. Notably, saposin D-deficient mice show an accumulation of ceramides containing α-hydroxy fatty acids in the kidney and cerebellum, but do not recapitulate the phenotypic abnormalities of human Farber disease (Matsuda *et al.*, 2004, 2007). The acid ceramidase reaction is also implicated in several human cancers, type 2 diabetes and Alzheimer's disease (Klein *et al.*, 1994; Park & Schuchman, 2006).

The four human saposin proteins (A, B, C and D) are small homologous nonenzymatic heat-stable and pH-stable glycoproteins. Saposin D has 34, 21 and 35% sequence identity to saposins A, B and C, respectively. The crystal and NMR structures of saposins A, B and C revealed conserved features, including six invariable cysteine residues that form three intrachain disulfide bridges over four amphipathic α-helices (Ahn, Faull, Whitelegge, Fluharty *et al.*, 2003; de Alba *et al.*, 2003; Ahn *et al.*, 2006; John *et al.*, 2006). In saposins A and C

the structures are compact monomers with a small hydrophobic core, similar to the structure of other saposin-like proteins (Liepinsh *et al.*, 1997; Bruhn, 2005). In contrast, the chain in saposin B opens up into a 'V' shape and associates into a tight homodimer that forms a large hydrophobic pocket for lipid binding (Ahn, Faull, Whitelegge, Fluharty *et al.*, 2003). Structural superpositions of saposins A, B and C show that the changes in the structure of the proteins arise from flexibility at three sites: 'hinges' in the loops between helices $\alpha1/\alpha2$ and $\alpha3/\alpha4$ and a kink in helix $\alpha3$ (Ahn *et al.*, 2006). Variability in the monomeric saposin conformation results in changes in the tertiary and quaternary structure which are directly related to their mode of action (Ahn, Faull, Whitelegge, Fluharty *et al.*, 2003; Ahn *et al.*, 2006; Bruhn, 2005; Hawkins *et al.*, 2005).

Here, we report the structure of saposin D in two different crystal forms. These structures were obtained at basic, neutral and acidic pH and show a typical monomeric compact saposin fold, with no significant conformational changes between the six crystallographically independent views of the protein. We highlight structural similarities as well as some interesting differences that distinguish saposin D from the other saposins.

2. Materials and methods

2.1. Protein expression and purification

The cloning, expression and purification protocols for saposin D were similar to previously reported methods (Ahn, Faull, Whitelegge, Higginson *et al.*, 2003; Ahn *et al.*, 2006). Briefly, the saposin D coding region was amplified from a partial pro-saposin cDNA (I.M.A.G.E. 3,615,413) by the polymerase chain reaction with primers that created 5′-*Nco*I and 3′-*Bam*HI sites. The amplified fragments encoded N-terminal Met and Gly residues, but otherwise no additional non-natural amino acids were included in the final coding region. The amplified fragment was digested and inserted into the pET-16 expression vector (Novagen). The resulting saposin D vector was used to transform *Escherichia coli* Rosetta gami-2 (DE3) cells (Novagen). Transformants were grown at 310 K in Terrific Broth to an OD_{600} of 0.6–0.8, induced with 0.8 m*M* isopropyl β-D-1-thiogalactopyranoside and grown for an additional 3 h before harvesting by centrifugation. Cells were resuspended in anion-exchange column binding buffer (25 m*M* NaCl, 25 m*M* Tris–HCl pH 7.0) and lysed by sonication. The lysates were subjected to centrifugation at 26 000*g* for 30 min and the supernatants were then heated at 358 K for 10 min followed by another round of centrifugation. The resulting supernatant was applied directly onto a Q-Sepharose column (BioRad) that had been pre-equilibrated in binding buffer and bound protein was eluted with a linear gradient of elution buffer (1 *M* NaCl, 25 m*M* Tris–HCl pH 7.0). The peak fractions containing saposin D were pooled, concentrated and applied onto a Superdex-75 size-exclusion column in 50 m*M* Tris–HCl buffer pH 7.0. Pooled saposin D fractions were exchanged into water and concentrated to 1.0 mg ml^{-1} and stored at 277 K. Samples were concentrated to 15 mg ml^{-1} immediately prior to crystallization. The mass of the final product as measured by MALDI–TOF mass spectrometry was within 0.01% of the calculated mass, assuming an N-terminal formylmethionine and three internal disulfide bonds (measured weight 9129.3 Da; calculated weight 9128.6 Da).

2.2. Crystallization and structure determination

Orthorhombic crystals of saposin D were grown at room temperature by vapour diffusion by mixing 1 µl of 15 mg ml^{-1} saposin D solution with 1 µl of a reservoir solution containing 0.15 *M* Tris–HCl pH 8.5, 0.2 *M* magnesium chloride and 32%(*w*/*v*) PEG 4000. The same crystal form was obtained using 0.1 *M* magnesium acetate, 0.15 *M* sodium cacodylate pH 6.5 and 32%(*w*/*v*) PEG 4000 or 0.1 *M* sodium acetate pH 4.6 and 22%(*w*/*v*) PEG 8000. Crystals were soaked in 1 *M* NaBr for 1 min for SAD phasing. Both native and NaBr-derivative crystals of saposin D were cryoprotected with 5%(*v*/*v*) ethylene glycol prior to flash-cooling. Crystals formed in the orthorhombic space group $P2_12_12_1$, with unit-cell parameters a = 40.45, b = 61.45, c = 64.57 Å. Diffraction data were collected at 100 K on beamline 19-ID at the Structural Biology Center, Advanced Photon Source, Argonne National Laboratory with an ADSC Quantum 315 CCD detector and were reduced using the *HKL*-3000 package (Minor *et al.*, 2006). For the NaBr-derivative data set, 480 oscillation images were collected with a rotation range of 1.0° per image and an exposure time of 3 s per image at a crystal-to-detector distance of 250 mm. For the native data set, two sets of 360 images were collected at crystal-to-detector distances of 150 and 400 mm. In both cases, oscillation images were collected with a rotation range of 0.5° per image with an exposure time of 3 s per image. The initial data analysis and SAD phasing were performed on the NaBr-derivative data with the *SHELXC*, *SHELXD* and *SHELXE* programs using the *HKL2MAP* graphical interface (Pape & Schneider, 2004). Model building and refinement was continued using the native data set using *ARP*/*wARP* (Morris *et al.*, 2003), *REFMAC*5 (Murshudov *et al.*, 1997), *SHELX*97 (Sheldrick, 2008) and *Coot* (Emsley & Cowtan, 2004). Two saposin D molecules were present in the asymmetric unit. The side chains for residues Lys21, Asn22, Lys34 and Glu64 of chain *A*, and Glu20, Lys21 and Asn22 of chain *B* had weak electron density and were not included in the final model.

The triclinic crystal form of saposin D was obtained using a reservoir solution consisting of 0.1 *M* sodium acetate pH 4.6, 0.2 *M* zinc sulfate and 30%(*w*/*v*) PEG 4000. Crystals were cryoprotected with 10%(*v*/*v*) ethylene glycol and native data were collected from a flash-cooled crystal at 100 K with Cu $K\alpha$ radiation on a Bruker Microstar X8 Proteum SMART CCD system. Two sets of 720 images were collected from different orientations of the crystal in the X-ray beam at a crystal-to-detector distance of 40 mm with a rotation range of 0.5° per image and 60 s exposure times. The diffraction data were reduced using the *PROTEUM* suite of programs. Crystals formed in space group *P*1, with unit-cell parameters a = 40.66, b = 41.12, c = 65.45 Å, α = 89.9, β = 81.2, γ = 71.4°. The structure was solved by molecular replacement with *Phaser*

Table 1
Data-collection statistics.

Values in parentheses are for the highest resolution shell.

	$P2_12_12_1$ (NaBr derivative)	$P2_12_12_1$ (native)	$P1$
Wavelength (Å)	0.9199	1.033	1.542
Resolution range (Å)	50–1.9 (1.94–1.90)	45–1.3 (1.35–1.30)	65–2.0 (2.05–2.00)
Completeness (%)	99.9 (99.2)	99.1 (98.1)	92.6 (91.2)
Wilson B factor (Å^2)	16.1	12.9	21.5
Redundancy	10.2 (10.1)	7.5 (6.5)	3.52 (1.4)
Mosaicity (°)	0.27	0.17	0.51
$R_{\rm merge}$	7.0 (28.0)	4.4 (21.8)	5.6 (13.9)
$\langle I\rangle/\langle\sigma(I)\rangle$	35.0 (8.6)	35.4 (8.1)	20.4 (6.7)

(McCoy *et al.*, 2007) using a single saposin D model from the orthorhombic structure as a search model. A total of four saposin D molecules were located. Model building and refinement were carried out using *ARP*/*wARP* (Morris *et al.*, 2003), *REFMAC*5 (Murshudov *et al.*, 1997) and *Coot* (Emsley & Cowtan, 2004). The side chains of residues Glu20 and Lys21 of chain *A*, Lys21 of chain *B*, Glu20, Lys21 and Lys34 of chain *C*, and Lys21, Asn22, Asn26 and Lys34 of chain *D* had weak electron density and were not included in the final model.

2.3. Structure analysis

Structure superpositions were calculated with *Swiss-PdbViewer* (Guex & Peitsch, 1997) and *ESCET* (Schneider, 2000). Protein structure images were produced with *PyMOL* (DeLano Scientific). Atomic coordinates and diffraction data have been deposited with the PDB with access codes 3bqp and 3bqq for the orthorhombic and triclinic forms, respectively.

3. Results and discussion

3.1. Expression, purification and crystallization

We previously reported a recombinant expression system for saposin B (Ahn, Faull, Whitelegge, Higginson *et al.*, 2003) that was adapted to the production of human saposins A and C (Ahn *et al.*, 2006). We obtained poor expression levels of human saposin D in this system, but found that the expression levels of saposin D improved to ∼3 mg per litre of cell culture using the Rosetta-gami 2 (DE3) strain of *E. coli*. This strain alleviates codon bias and provides an oxidizing environment that promotes disulfide-bond formation within the cytoplasm. Similar to our results with saposins A, B and C, we purified saposin D without any additional purification tags through sequential steps of cell lysis, heating, differential centrifugation, ion-exchange and gel-filtration chromatography (Ahn, Faull, Whitelegge, Higginson *et al.*, 2003; Ahn *et al.*, 2006).

Our final purified sample of saposin D produced X-ray diffraction-quality crystals under several crystallization conditions ranging in pH from 8.5 to 4.6 (see §2). Ultimately, we determined the structures of saposin D from an orthorhombic crystal form grown at pH 8.5 with two copies of the protein per asymmetric unit and a triclinic crystal form grown at pH 4.6 with four crystallographically independent chains (Tables 1 and 2).

3.2. General description of the saposin D structure

Both crystal structures of saposin D revealed a typical monomeric saposin fold of four amphipathic α-helices (α1, residues Cys5–Arg17; α2, residues Lys25–Ser37; α3, residues Asp41–Val63; α4, residues Pro68–Lys74) forming an ellipsoid with approximate dimensions 29 × 28 × 17 Å (Fig. 1*a*). Similar to the crystal structures of saposins A and C, saposin D shows a compact monomeric saposin fold with a packed hydrophobic core, in contrast to the large internal cavity seen in the saposin B homodimer (Ahn, Faull, Whitelegge, Fluharty *et al.*, 2003). Consistent with an earlier mapping of the disulfide topology in saposin D (Tatti *et al.*, 1999), helices α1 and α4 of the 80-residue protein are joined by disulfide bonds between cysteines 5/78 and 8/72 in the 'stem' region of the protein (helices α1 and α4) and 36/47 in the 'hairpin' region (helices α2 and α3). All six crystallographic structures of the

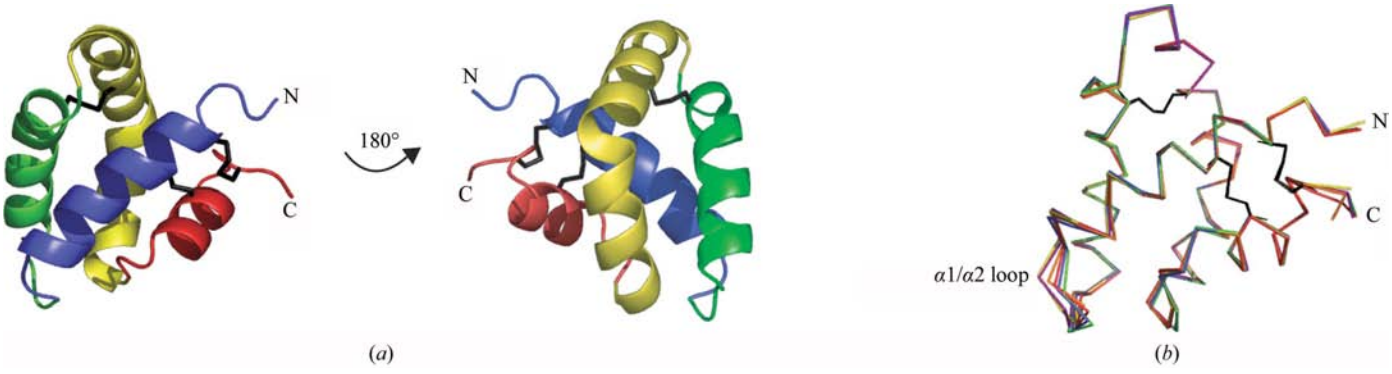

Figure 1
Structure of saposin D. (*a*) Ribbon representation of saposin D with helices α1, α2, α3 and α4 coloured blue, green, yellow and red, respectively. Disulfide bonds are indicated by black lines. (*b*) Superposition of the two molecules from the orthorhombic form (red and orange) and the four molecules from the triclinic form (yellow, green, blue and purple).

Table 2
Refinement statistics.

	$P2_12_12_1$	$P1$
Resolution range (Å)	35–1.30	65–2.0
No. of reflections, working set	36313	23121
No. of reflections, test set	2010	1308
R_{work}/R_{free} (5%)	17.6/23.4	19.5/24.2
No. of protein chains	2	4
No. of protein atoms	1271	2477
No. of waters	198	314
No. of magnesium ions	3	0
Average protein *B* factor (Å^2)	22.2	20.5
Average water *B* factor (Å^2)	32.9	28.8
R.m.s.d. bond lengths (Å)	0.011	0.013
R.m.s.d. bond angles (°)	2.1	1.4

protein were highly similar, with pairwise C$^\alpha$ r.m.s.d. values ranging from 0.21 to 0.57 Å over all residues, with the exclusion of residues 20 and 21 from the $\alpha1/\alpha2$ loop (78 atoms; Fig. 1*b*). This loop has slight deviations between the six copies of saposin D and this region of the protein is not involved in crystal lattice contacts in any of the structures. This loop is of interest because it includes the Asn22 site of glycosylation in the natural protein. Our protein was produced in *E. coli* and is thus not glycosylated.

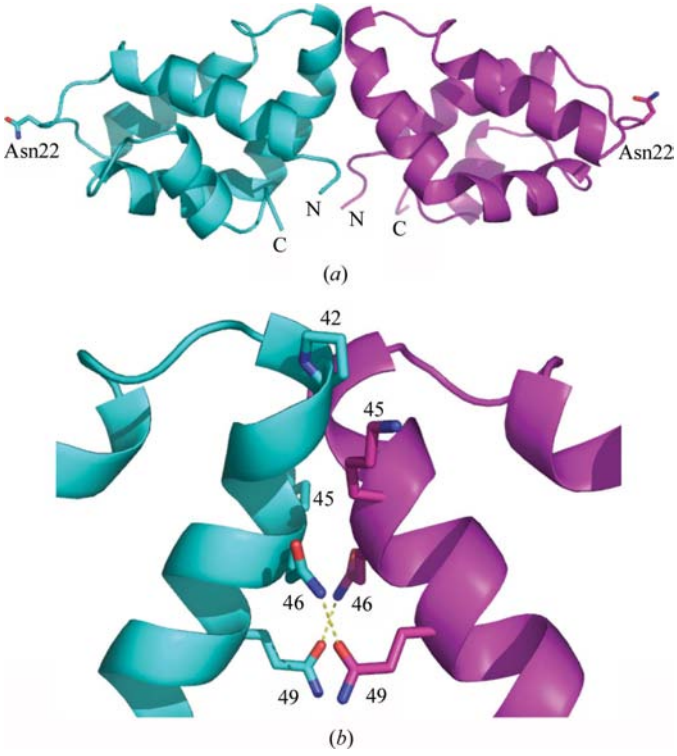

Figure 2
Putative dimer of saposin D. (*a*) Ribbon representation of the association between chains *A* and *B* in the triclinic crystal form. Similar dimers are observed between chains *C* and *D* in the triclinic form and between chains *A* and *B* in the orthorhombic form. The conserved glycosylation site at residue Asn22 is indicated. (*b*) Close-up view of the interchain contact surface. Residues Pro42, Lys45, Gln46 and Gln49 are indicated. The dotted lines represent interchain hydrogen bonds between residues Gln46 and Gln49.

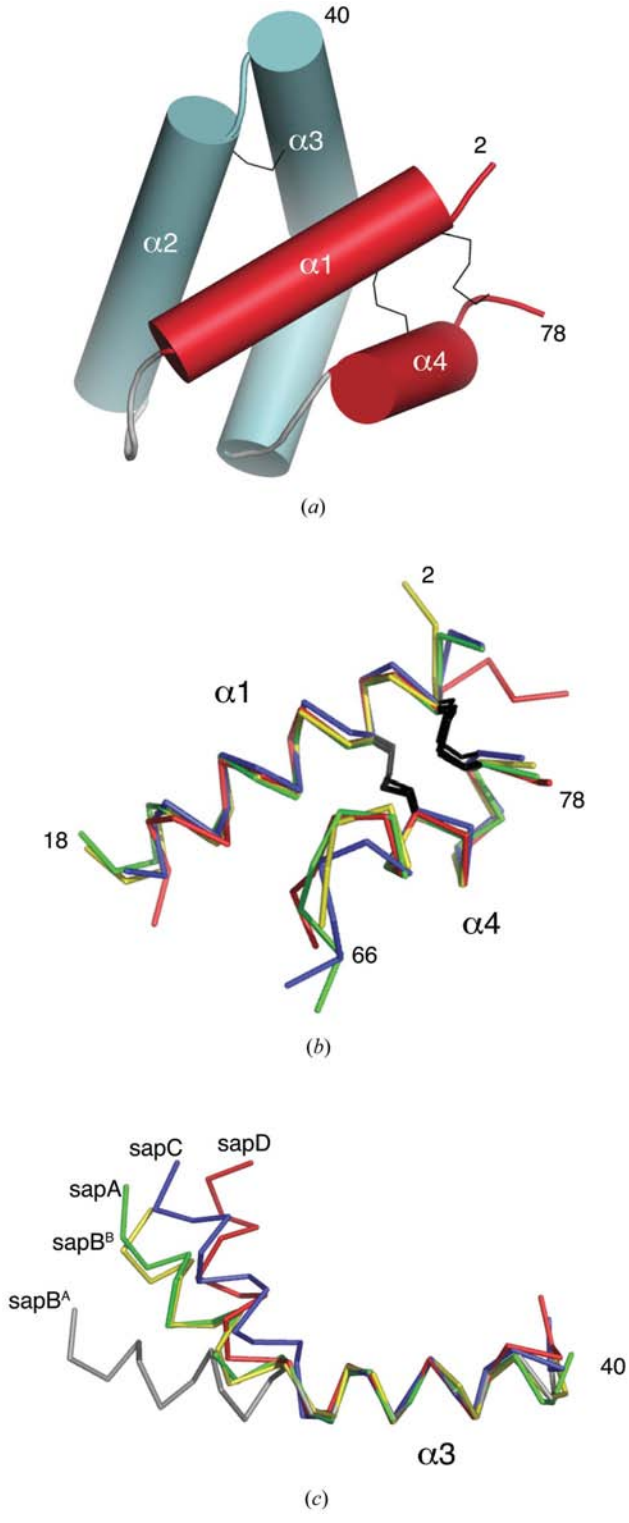

Figure 3
Structural comparison of the four saposins. (*a*) The saposin D structure coloured according to the stem (red) and hairpin (blue) regions. (*b*) Superposition of the stem (helices $\alpha1$ and $\alpha4$) regions of the four human saposins (PDB codes 2dob, 1n69 and 2gtg for saposins A, B and C, respectively). Saposins A, B (chain *B*), C and D are coloured green, yellow, blue and red, respectively. Disulfide bonds are indicated in black. (*c*) Residues 40–65, following the superposition of residues 43–54 of helix $\alpha3$ from the hairpin region. The variable kink in the four saposins is localized at Tyr54. The C$^\alpha$ traces are coloured as in (*b*), with the exception of the grey helix, which is from chain *A* of saposin B.

The membrane-binding and hydrolase-activation functions of the saposins are highly dependent on pH and are optimal at the pH of the late lysosome (∼4.8; Azuma *et al.*, 1994; Vaccaro *et al.*, 1995; Kolter & Sandhoff, 2005; Alattia *et al.*, 2007). In particular, the lipid-binding and sphingolipid-activation function of saposin D requires an acidic pH and the presence of anionic phospholipids (Tatti *et al.*, 1999; Ciaffoni *et al.*, 2001, 2003; Linke *et al.*, 2001). pH changes alone do not generally result in large conformational changes in the saposins in solution, although pH has an important effect on their lipid-binding properties (de Alba *et al.*, 2003; Hawkins *et al.*, 2005; Ahn *et al.*, 2006; John *et al.*, 2006). An exception is saposin C, for which a dimeric form may be thermodynamically more stable at pH 4.0 (John *et al.*, 2006). We obtained the orthorhombic crystal form of saposin D at basic, neutral and acidic pH values and since all had similar unit-cell parameters, the structures of saposin D in all crystals are similar. John *et al.* (2006) have reported two conformations of monomeric saposin D at neutral and acidic pH values and our crystals may have selected for one of these states. The high similarity between the structures of all six chains from the orthorhombic and triclinic forms (Fig. 1*b*) establish that the observed conformation of saposin D in these crystals is not significantly affected by lattice contacts.

3.3. Dimers

Both the orthorhombic and triclinic crystal forms of saposin D reveal similar dimer associations involving noncrystallographic pseudo-twofold axes. There are nonpolar and hydrogen-bond interactions between adjacent chains between residues Pro42, Lys45, Gln46 and Gln49 of α3 and Gly3 of the N-terminus (Fig. 2). Given the small buried surface area of ∼450 Å^2, we cannot rule out that this is simply a crystal lattice contact that has no relevance in solution (Bahadur *et al.*, 2004). In fact, we have only observed saposin D monomers in solution by size-exclusion gel-filtration chromatography and dynamic light scattering (data not shown). However, this interaction may represent a weak biological interface since it is independently observed three times in the two crystal forms. Although our solution studies do not support the crystallographically observed saposin D dimer, this does not exclude the possibility of a weak interaction occurring *in vivo*. Similar interchain associations involving helix α3 are not observed in the crystal structures of saposins A, B or C. Saposin arrays on membrane surfaces sustained by homomeric protein–protein contacts have been previously described for saposin C in our laboratory (Alattia *et al.*, 2006).

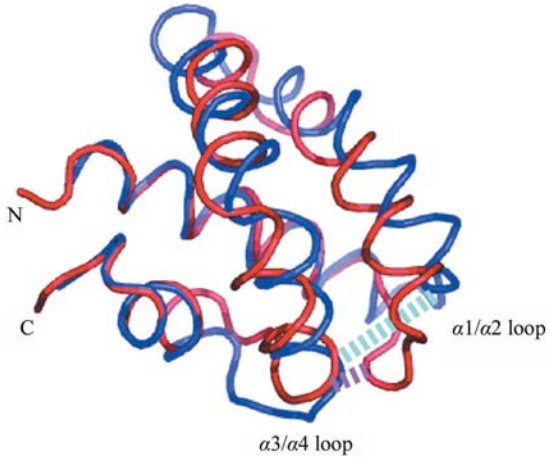

Figure 4
Superposition of the stem region of saposin C (blue) and saposin D (red), showing a relative displacement of the hairpin. The dashed lines indicate the distance between the α1/α2 and α3/α4 loops in the two structures.

3.4. Comparison with saposins A, B and C

The four human saposins differ in their membrane interactions, sphingolipid specificities and most likely in their mode of action (Kolter & Sandhoff, 2005), and the flexibility in the saposin structures is likely to be important in sphingolipid activation (Ahn, Faull, Whitelegge, Fluharty *et al.*, 2003; Hawkins *et al.*, 2005; Ahn *et al.*, 2006; Stokeley *et al.*, 2007). We have previously described 'hinge' areas in the α1/α2 and α3/α4 loops as flexible points connecting the stem (α1 + α4) and hairpin (α2 + α3) regions of the saposins (Ahn, Faull, Whitelegge, Fluharty *et al.*, 2003; Ahn *et al.*, 2006; Fig. 3*a*). Individually, the stem and hairpin regions superpose well between members of the saposin family; however, differences in the relative orientations of these two regions can result in large global conformational changes (Ahn *et al.*, 2006). An important third point of structural variability is present in α3, which has been observed in kinked forms in saposins A, B and C (Ahn, Faull, Whitelegge, Fluharty *et al.*, 2003; de Alba *et al.*, 2003; Ahn *et al.*, 2006) and in an unkinked conformation in unliganded saposin B dimers (Ahn, Faull, Whitelegge, Fluharty *et al.*, 2003) and SDS-bound saposin C (Hawkins *et al.*, 2005).

With the structure of saposin D in hand, we can now complete the structural comparisons of the four saposins. The stem regions of all four saposin proteins superimpose very well, with r.m.s.d. values ranging from 0.47 to 0.59 Å for the 21 C$^\alpha$ atoms of residues 5–17 and 71–78 (saposin D numbering; Fig. 3*b*). The hairpin region is not as consistently regular between the saposins and saposin D agrees most closely with saposin C in this region, with a C$^\alpha$ r.m.s.d. of 0.85 Å for residues 24–54, comprising α2, the α2/α3 loop and the N-terminal half of α3 (31 atoms). The kink in helix α3 at or near residue Tyr54 (Ahn *et al.*, 2006) is more pronounced in saposin D. The axis kink is approximately 52° in saposin A and saposin B (chain *B*), 64° in saposin C and 75° in saposin D (Fig. 3*c*). In chains *A* and *C* of the saposin B crystal structure (Ahn, Faull, Whitelegge, Fluharty *et al.*, 2003), helix α3 is not kinked but is slightly curved (shown as a grey C$^\alpha$ trace in Fig. 3*c*). In addition to the two hinge-loop regions, the reversible kinking of this helix is one of the key areas of the fold responsible for variability in saposin structures. These structural changes are associated with lipid-substrate binding and/or membrane–detergent association (Ahn, Faull, Whitelegge, Fluharty *et al.*, 2003; Bruhn, 2005; Hawkins *et al.*, 2005).

Saposin D is most structurally similar to saposin C, but an overall C^{α} superposition gives a poor fit, with an r.m.s.d. value of 2.6 Å over residues 2–79. Inspection of the backbone dihedral angles shows that saposins D and C mainly differ in the two hinge loops (residues 20–23 and 65–67) and in the sharper kink in α3. This results in a reorientation of the hairpin relative to the stem (Fig. 4). One consequence of the reorganization is that the distance between the α1/α2 and the α3/α4 loops is approximately 10 Å in saposin D, whereas the distances are 19, 18 and 17 Å in saposins A, B and C, respectively.

4. Summary

The crystal structure of saposin D closely resembles the previously determined structures of the monomeric saposins A and C, as opposed to the saposin B dimer. There are differences in the two hinge regions and in the α3 kink site of the four saposins and these sites indicate flexibility that may result in larger changes that occur upon association with lipids or lipid bilayers. Similar interchain contacts are seen in the two different crystal forms, but the protein is monomeric in solution, indicating that saposin D may have a weak propensity for dimerization. A more complete description of the saposin activation reaction will require the characterization of the membrane-induced structural changes in each of the four saposins.

This work was supported by a CIHR grant to GGP. We thank Lu Chen for preparing the saposin D expression vector. The results shown in this report are derived from work performed at Argonne National Laboratory, Structural Biology Center beamline 19ID at the Advanced Photon Source. Argonne is operated by UChicago Argonne, LLC for the US Department of Energy, Office of Biological and Environmental Research under contract DE-AC02-06CH11357.

References

Ahn, V. E., Faull, K. F., Whitelegge, J. P., Fluharty, A. L. & Privé, G. G. (2003). *Proc. Natl Acad. Sci. USA*, **100**, 38–43.
Ahn, V. E., Faull, K. F., Whitelegge, J. P., Higginson, J., Fluharty, A. L. & Privé, G. G. (2003). *Protein Expr. Purif.* **27**, 186–193.
Ahn, V. E., Leyko, P., Alattia, J. R., Chen, L. & Privé, G. G. (2006). *Protein Sci.* **15**, 1849–1857.
Alattia, J. R., Shaw, J. E., Yip, C. M. & Privé, G. G. (2006). *J. Mol. Biol.* **362**, 943–953.
Alattia, J. R., Shaw, J. E., Yip, C. M. & Privé, G. G. (2007). *Proc. Natl Acad. Sci. USA*, **104**, 17394–17399.
Alba, E. de, Weiler, S. & Tjandra, N. (2003). *Biochemistry*, **42**, 14729–14740.
Azuma, N., O'Brien, J. S., Moser, H. W. & Kishimoto, Y. (1994). *Arch. Biochem. Biophys.* **311**, 354–357.
Bahadur, R. P., Chakrabarti, P., Rodier, F. & Janin, J. (2004). *J. Mol. Biol.* **336**, 943–955.
Bruhn, H. (2005). *Biochem. J.* **389**, 249–257.
Ciaffoni, F., Salvioli, R., Tatti, M., Arancia, G., Crateri, P. & Vaccaro, A. M. (2001). *J. Biol. Chem.* **276**, 31583–31589.
Ciaffoni, F., Tatti, M., Salvioli, R. & Vaccaro, A. M. (2003). *Biochem. J.* **373**, 785–792.
Emsley, P. & Cowtan, K. (2004). *Acta Cryst.* D**60**, 2126–2132.
Futerman, A. H. & van Meer, G. (2004). *Nature Rev. Mol. Cell Biol.* **5**, 554–565.
Guex, N. & Peitsch, M. C. (1997). *Electrophoresis*, **18**, 2714–2723.
Hawkins, C. A., de Alba, E. & Tjandra, N. (2005). *J. Mol. Biol.* **346**, 1381–1392.
John, M., Wendeler, M., Heller, M., Sandhoff, K. & Kessler, H. (2006). *Biochemistry*, **45**, 5206–5216.
Klein, A., Henseler, M., Klein, C., Suzuki, K., Harzer, K. & Sandhoff, K. (1994). *Biochem. Biophys. Res. Commun.* **200**, 1440–1448.
Kolter, T. & Sandhoff, K. (2005). *Annu. Rev. Cell. Dev. Biol.* **21**, 81–103.
Liepinsh, E., Andersson, M., Ruysschaert, J. M. & Otting, G. (1997). *Nature Struct. Biol.* **4**, 793–795.
Linke, T., Wilkening, G., Sadeghlar, F., Mozcall, H., Bernardo, K., Schuchman, E. & Sandhoff, K. (2001). *J. Biol. Chem.* **276**, 5760–5768.
McCoy, A. J., Grosse-Kunstleve, R. W., Adams, P. D., Winn, M. D., Storoni, L. C. & Read, R. J. (2007). *J. Appl. Cryst.* **40**, 658–674.
Matsuda, J., Kido, M., Tadano-Aritomi, K., Ishizuka, I., Tominaga, K., Toida, K., Takeda, E., Suzuki, K. & Kuroda, Y. (2004). *Hum. Mol. Genet.* **13**, 2709–2723.
Matsuda, J., Yoneshige, A. & Suzuki, K. (2007). *J. Neurochem.* **103**, *Suppl.* 1, 32–38.
Minor, W., Cymborowski, M., Otwinowski, Z. & Chruszcz, M. (2006). *Acta Cryst.* D**62**, 859–866.
Morris, R. J., Perrakis, A. & Lamzin, V. S. (2003). *Methods Enzymol.* **374**, 229–244.
Murshudov, G. N., Vagin, A. A. & Dodson, E. J. (1997). *Acta Cryst.* D**53**, 240–255.
Pape, T. & Schneider, T. R. (2004). *J. Appl. Cryst.* **37**, 843–844.
Park, J. H. & Schuchman, E. H. (2006). *Biochim. Biophys. Acta*, **1758**, 2133–2138.
Sandhoff, K. & Kolter, T. (2003). *Philos. Trans. R. Soc. Lond. B Biol. Sci.* **358**, 847–861.
Schneider, T. R. (2000). *Acta Cryst.* D**56**, 714–721.
Sheldrick, G. M. (2008). *Acta Cryst.* A**64**, 112–122.
Stokeley, D., Bemporad, D., Gavaghan, D. & Sansom, M. S. (2007). *Biochemistry*, **46**, 13573–13580.
Tatti, M., Salvioli, R., Ciaffoni, F., Pucci, P., Andolfo, A., Amoresano, A. & Vaccaro, A. M. (1999). *Eur. J. Biochem.* **263**, 486–494.
Vaccaro, A. M., Ciaffoni, F., Tatti, M., Salvioli, R., Barca, A., Tognozzi, D. & Scerch, C. (1995). *J. Biol. Chem.* **270**, 30576–30580.
Watts, R. W. (2003). *Philos. Trans. R. Soc. Lond. B Biol. Sci.* **358**, 975–983.